Measurement of the Rare Decay $\pi^0 \rightarrow e^+e^-$

R. E. Mischke, J. S. Frank, C. M. Hoffman, D. C. Moir,
J. S. Sarracino, and P. A. Thompson[a]
Los Alamos National Laboratory, Los Alamos, New Mexico 87545

and

M. A. Schardt[b]
Department of Physics, Arizona State University, Tempe, Arizona 85281, and
Los Alamos National Laboratory, Los Alamos, New Mexico 87545

(Received 18 February 1982)

Evidence for the rare decay $\pi^0 \rightarrow e^+e^-$ has been obtained in an experiment which measured the invariant mass spectrum of e^+e^- pairs produced by 300-MeV/c π^- mesons interacting in a liquid-hydrogen target. The branching ratio is $(1.8 \pm 0.6) \times 10^{-7}$, about four times larger than the unitarity lower limit.

PACS numbers: 13.20.Cz, 14.40.Aq

This paper reports a measurement of the branching ratio for the rare decay $\pi^0 \rightarrow e^+e^-$. Like other pseudoscalar mesons that decay into lepton pairs, this one can proceed through an intermediate state of two virtual photons. The contribution from this process dominates the imaginary part of the amplitude for the decay. This implies a lower bound on the branching ratio called the unitarity lower limit,[1,2] which is found to be $B = \Gamma(\pi^0 \rightarrow e^+e^-)/\Gamma(\pi^0 \rightarrow \gamma\gamma) \geq 0.48 \times 10^{-7}$. The first calculation of the real part of the amplitude was by Drell[3] in 1959. Since then, many models have been used to estimate B. The effects of vector dominance,[2,4] baryon loops,[5] direct quark-lepton coupling,[6-8] weak neutral currents,[9,10] and Higgs bosons[11,12] have been included by different authors. In general, most results predict only small enhancements over the unitarity lower limit. In addition to two experimental upper limits,[7,13] there has been one measurement[14] of the branching ratio with the result $B = (2.2^{+2.4}_{-1.1}) \times 10^{-7}$.

Our experiment was performed at the Clinton P. Anderson Meson Physics Facility (LAMPF) using a beam of 1.8×10^7 π^-/s with a momentum of 300 MeV/c. The pion flux was monitored by an ionization chamber and scintillation counter telescopes.[15] The production of neutral pions was through the reaction $\pi^- p \rightarrow \pi^0 n$ in a 5-cm-diam and 25-cm-long liquid-hydrogen target. Most e^+e^- pairs coming from the target resulted from π^0 decays, often with a photon being converted through Compton scattering or pair production. In principle, these pairs always have an effective mass less than M_{π^0} because some energy from the π^0 is carried away by undetected e^+, e^-, or photons. Another source of lepton pairs was the reaction $\pi^- p \rightarrow n e^+ e^-$; here the effective mass of the pair ranges from near zero to 410 MeV/c^2.

The e^+ and e^- were identified and momentum analyzed in the magnetic spectrometer shown in Fig. 1. Multiwire proportional chambers (MWPC) were placed both upstream and downstream of a large aperture magnet. Behind the chambers, a row of scintillation counters detected a charged particle on each side of the beam line and a gas Cherenkov counter provided identification of electrons. In the center of the magnet a uranium plug stopped the incident pions to prevent a high flux of particles in the rear chambers. The acceptance of the spectrometer was optimized for the kinematics of forward-produced π^0's with the e^+ and e^- transverse to the π^0 direction in the π^0 rest frame.

A total of 2.4×10^{13} incident π^- produced ~50 000

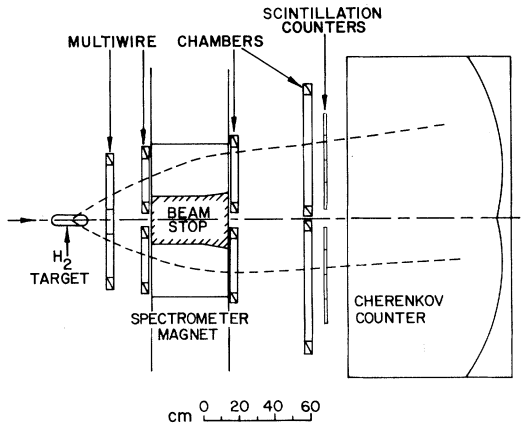

FIG. 1. Top view of apparatus. The incident π^- beam enters from the left and interacts in the target. The resulting e^+e^- from π^0 decay are detected by the multiwire chambers and scintillation and Cherenkov counters.

candidate events. Each candidate included hits in at least three of the four chamber planes in both the horizontal and vertical coordinates on each side. A reconstruction program took the locations of hits recorded by the MWPC planes and considered all plausible combinations to find the best-fit trajectories through the spectrometer. About one third of the candidate events contained two acceptable tracks. For each such event the two trajectories were extrapolated upstream to find their point of closest approach and to calculate the effective mass M of the pair. Cuts were applied to define a fiducial volume for the apparatus and to help eliminate accidental coincidences. Acceptable events were required to originate within the volume of the target. A cut requiring the sum of the e^+ and e^- energies to be >290 MeV eliminated most events in which undetected particles carried off a significant amount of energy from the decay.

The remaining data sample contained 1330 events whose effective mass distribution is shown in Fig. 2(a). This spectrum consists of four components: The signal from $\pi^0 \to e^+e^-$ which is clustered near $M_{\pi^0}{}^2$, the background from other π^0 decay modes which dominates the mass region below and up to $M_{\pi^0}{}^2$, and relatively flat contributions from accidentals and from the reaction $\pi^- p \to n e^+ e^-$. The accidentals spectrum shown in Fig. 2(c) was obtained by combining tracks from different data events.

A Monte Carlo simulation of the experiment was performed to determine the shape of the spectrum of the square of the effective mass for the other three components. The simulation reproduced the dynamics and kinematics of each process as well as the geometry of the experiment. The effects of multiple scattering, energy loss, chamber resolution, and inefficiencies were included. The program generated simulated hits in the chambers; these were processed by the same programs used for the data analysis. The resulting spectrum for the $\pi^0 \to e^+e^-$ mode shown in Fig. 2(b) illustrates the mass resolution. The distribution for $\pi^- p \to n e^+ e^-$ in Fig. 2(d) indicates the shape of the mass acceptance of the apparatus since the input spectrum varies slowly with mass. The input spectrum for the other π^0 decay modes, which includes approximately equal contributions from external and internal conversion of photons, falls rapidly with increasing M^2 and ends at $M_{\pi^0}{}^2$. The resulting spectrum displayed in Fig. 2(e) extends slightly above $M_{\pi^0}{}^2$ as a result of the resolution of the apparatus and is truncated at lower M^2 by the cut which eliminated events with significant missing energy.

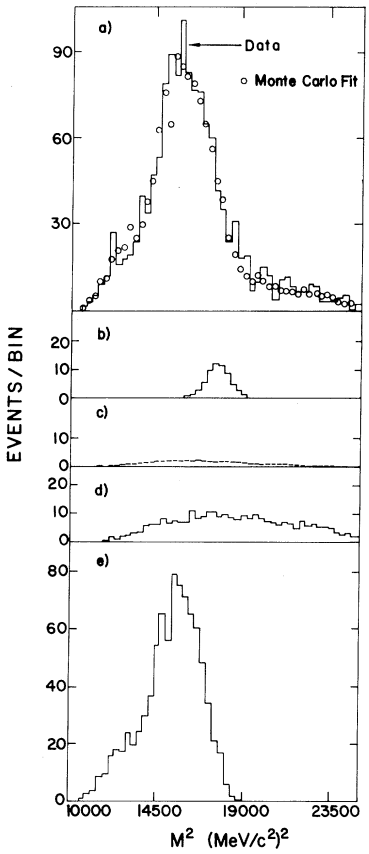

FIG. 2. (a) Final data sample showing number of events vs square of the effective mass. The open circles are the best normalization of the Monte Carlo spectra to the data. (b)–(e) Normalized Monte Carlo decomposition of contributions to the total number of events for (b) $\pi^0 \to e^+e^-$, (c) accidentals, (d) $\pi^- p \to n e^+ e^-$, and (e) other π^0 decay modes.

Several checks were made to ensure that the Monte Carlo simulation reproduced all essential aspects of the data sample. The distributions of χ^2 for the track fits were compared. The agreement was excellent for the 85% of the data with χ^2 values below 3 per degree of freedom (df), indicating correct simulation of chamber resolutions and multiple scattering. At large χ^2 there was an excess of data events due to omission of higher-order processes in the Monte Carlo simulation. We have verified that the results of this experiment are independent of what maximum-χ^2 cut was used. Another sensitive test of the simulation was the distribution of distance of closest approach of the two tracks. The width of this distribution was 6.6 mm full width at half maximum.

The width from the Monte Carlo simulation agrees to 10%, which confirms the extrapolation to a common origin for the events. The tails of the data distribution were used to calculate the number of accidental coincidences in the data sample to be $(5\pm1)\%$.

A χ^2 minimization routine adjusted the scale factors for the signal from $\pi^0\to e^+e^-$, the background from other π^0 decay modes, and the background from $\pi^-p\to ne^+e^-$ to obtain a best normalization of the Monte Carlo spectra to the data. The best fit is shown in Fig. 2(a) and has a χ^2 of 49.1 for 47 df. The statistical errors for both the data and the Monte Carlo spectra were included. The fit requires 58 ± 19 $\pi^0\to e^+e^-$ events. Fixing the $\pi^0\to e^+e^-$ signal to either 0 or 120 events increases the χ^2 to 57.2 for 48 df. The corresponding branching ratio can be obtained by normalizing to the contribution from the other π^0 decay modes or from the calculated number of π^0's produced and the known acceptance of the apparatus. The results are consistent and give $B=(1.8\pm0.6)\times10^{-7}$.

We have studied the stability of the $\pi^0\to e^+e^-$ signal to possible uncertainties in various parameters. The absolute momentum scale is known with an uncertainty of 0.8% from a detailed map of the magnetic field and the measured locations of the chamber planes. This scale was confirmed at the 1% level from our knowledge of the beam momentum and the reconstructed momenta of elastically scattered pions; the contribution to the systematic error is negligible. The conversion probability, averaged over photon energy and material traversed, was $(1.96\pm0.05)\times10^{-3}$, which leads to a 2% systematic error in the $\pi^0\to e^+e^-$ signal. The fit assumed a netural-pion electromagnetic form-factor slope[16] $a=0.11\pm0.03$ for the Dalitz decay mode. The experimental error in the form-factor slope results in a 3% uncertainty in the $\pi^0\to e^+e^-$ signal. Removal of the cut on the sum of the two lepton energies raises the deduced $\pi^0\to e^+e^-$ signal by 6%. Finally, the uncertainty in the number of accidental coincidences in the data sample implies a 1% uncertainty in the $\pi^0\to e^+e^-$ signal.

In summary, we see statistically significant evidence for the decay $\pi^0\to e^+e^-$ which is insensitive to large changes in the event selection criteria and to assumptions concerning the background processes and strengths. We estimate an overall systematic uncertainty of less than 10%.

Visual evidence for the presence of a $\pi^0\to e^+e^-$ signal in the data is shown in Fig. 3. This figure shows the M^2 distribution of the difference between the data and the best fit to all modes excluding the region around $M_{\pi^0}{}^2$. There is a significant excess of data events with mass values near $M_{\pi^0}{}^2$. The normalized $\pi^0\to e^+e^-$ signal is superimposed on this spectrum.

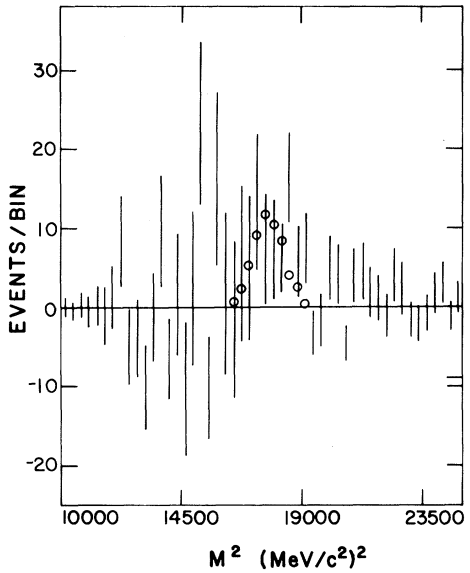

FIG. 3. Data minus Monte Carlo with $\pi^0\to e^+e^-$ signal region excluded from the fit. The open circles represent the signal of 58 $\pi^0\to e^+e^-$ events.

Our result is almost four times the unitarity lower limit. It is larger than expected from existing calculations. The earliest calculations for B were based on a dispersion relation with an arbitrary cutoff parameter required to avoid infinities.[1,3] The formulation[3] which is insensitive to the cutoff parameter predicts a value less than 10^{-7}. Other calculations used the vector dominance model[2,4]; these calculations also predict branching ratios smaller than 10^{-7} for reasonable assumptions. The contribution from weak neutral currents or massive Higgs bosons is expected to be negligible.[9-12] Thus it appears difficult to explain a branching ratio as large as 1.8×10^{-7}, but our experimental error is too large to exclude these calculations. Consequently, it is not necessary at this time to invoke anomalous lepton-quark couplings.[6-8]

We wish to thank the management and staff of LAMPF and our many colleagues who assisted in the execution of this experiment. This work was supported by the U. S. Department of Energy and Associated Western Universities, Inc.

[a]Present address: Brookhaven National Laboratory,

Upton, N.Y. 11973.
[b]Present address: Siemons Gammasonics, Inc., Des Plaines, Ill. 60018.
[1]S. M. Berman and D. A. Geffan, Nuovo Cimento 18, 1192 (1960).
[2]C. Quigg and J. D. Jackson, Lawrence Radiation Laboratory Report No. UCRL-18487, 1978 (unpublished).
[3]S. D. Drell, Nuovo Cimento 11, 693 (1959).
[4]I. K. Litskevich and V. A. Franke, Yad. Fiz. 10, 815 (1969) [Sov. J. Nucl. Phys. 10, 471 (1970)].
[5]M. Pratap and J. Smith, Phys. Rev. D 5, 2020 (1972).
[6]A. Soni, Phys. Lett. 52B, 332 (1974), and 53B, 280 (1974).
[7]J. D. Davies, J. G. Guy, and R. K. P. Zia, Nuovo Cimento A24, 324 (1974).
[8]J. C. Pati and A. Salam, Phys. Rev. D 11, 1137 (1975).
[9]F. C. Michel, Phys. Rev. 138, B408 (1965).
[10]P. Herczeg, Phys. Rev. D 16, 712 (1977).
[11]H. E. Haber, G. L. Kane, and T. Sterling, Nucl. Phys. B161, 493 (1979).
[12]P. Herczeg, private communication, and in Proceedings of the Workshop on Program Options in Intermediate Energy Physics, Los Alamos National Laboratory Report No. LA-8335-C, May 1980 (unpublished).
[13]J. Schacher *et al.*, Nuovo Cimento Lett. 20, 177 (1977).
[14]J. Fischer *et al.*, Phys. Lett. 73B, 364 (1978).
[15]M. A. Schardt *et al.*, Phys. Rev. D 23, 639 (1981).
[16]J. Fischer *et al.*, Phys. Lett. 73B, 359 (1978).

Axions, Domain Walls, and the Early Universe

P. Sikivie
Department of Physics, University of Florida, Gainesville, Florida 32611
(Received 8 February 1982)

Axion models have a spontaneously broken $Z(N)$ symmetry. The resulting discretely degenerate vacua and domain-wall solitons are incompatible with the standard cosmology. It is possible, however, to introduce a small $Z(N)$ breaking interaction into axion models without upsetting the Peccei-Quinn mechanism. In that case the domain walls disappear a certain time after their formation in the early universe. Their presence for a limited time period might lead to galaxy formation.

PACS numbers: 11.15.Ex, 11.30.Er, 12.10.En, 98.80.Bp

When a gauge interaction explicitly breaks a global symmetry, it often happens that a discrete subgroup of the global symmetry remains unbroken. Such is the case in axion models[1] which, as I am about to show, have a spontaneously broken $Z(N)$ symmetry. The result applies to all models which have a Peccei-Quinn symmetry $U_{PQ}(1)$ which is broken only by the QCD gluon anomaly. N is the number of quark flavors that rotate under $U_{PQ}(1)$. To be specific however, I analyze the Dine-Fischler-Srednicki model[2] in which the axion can be made "invisible." The Yukawa couplings and scalar self-interactions of that model,

$$-\sum_{i,j=1}^{N/2} K_i^{uj}(u_{Li}'^{\dagger} d_{Li}'^{\dagger})\begin{pmatrix}\varphi_1^0\\ \varphi_1^-\end{pmatrix} u_{Rj}' + \text{H.c.} - \sum_{i,j=1}^{N/2} K_i^{dj}(u_{Li}'^{\dagger} d_{Li}'^{\dagger})\begin{pmatrix}-\varphi_2^{-*}\\ \varphi_2^{0*}\end{pmatrix} d_{Rj}' + \text{H.c.} - V(\varphi_1, \varphi_2, \Phi), \quad (1)$$

have the $U_{PQ}(1)$ symmetry:

$$q_i \to e^{i\alpha\gamma_5} q_i, \quad \varphi_1 \to e^{-2i\alpha}\varphi_1,$$
$$\varphi_2 \to e^{+2i\alpha}\varphi_2, \quad \Phi \to e^{-2i\alpha}\Phi. \quad (2)$$

Φ is a singlet under the standard gauge group, which is coupled to φ_1 and φ_2 through V. $U_{PQ}(1)$ is explicitly broken by and only by the QCD gluon anomaly. The corresponding anomalous Ward identity requires the change

$$\theta_{QCD} \to \theta_{QCD} - 2N\alpha \quad (3)$$

when the transformation (2) is applied.

However, a $Z(N)$ subgroup of $U_{PQ}(1)$ remains unbroken. Indeed, consider the subgroup $Z_L(N) \otimes Z_R(N) \otimes U_V(1)$ of the global symmetry group $SU_L(N) \otimes SU_R(N) \otimes U_V(1)$ of QCD[3]:

$$q_{Li} \to \exp[i(2\pi k_L/N + \beta)]\, q_{Li},$$
$$q_{Ri} \to \exp[i(2\pi k_R/N + \beta)]\, q_{Ri}, \quad (4)$$

where k_L and k_R are integers. These are also symmetries of the $SU_L(2) \otimes U_Y(1)$ gauge interactions and indeed of the full theory provided that